

# Charged Fullerenes as High-Capacity Hydrogen Storage Media

Mina Yoon,<sup>\*,†,‡</sup> Shen Yuan Yang,<sup>‡,§</sup> Enge Wang,<sup>§</sup> and Zhenyu Zhang<sup>†,‡</sup>

*Materials Science and Technology Division, Oak Ridge National Laboratory, Oak Ridge, Tennessee 37831, Department of Physics and Astronomy, The University of Tennessee, Knoxville, Tennessee 37996, and International Center for Quantum Structures and Institute of Physics, Chinese Academy of Sciences, Beijing 100080, China*

Received April 5, 2007; Revised Manuscript Received July 2, 2007

## ABSTRACT

Using first-principles calculations within density functional theory, we explore systematically the capacity of charged carbon fullerenes  $C_n$  ( $20 \leq n \leq 82$ ) as hydrogen storage media. We find that the binding strength of molecular hydrogen on either positively or negatively charged fullerenes can be dramatically enhanced to 0.18–0.32 eV, a desirable range for potential room-temperature, near ambient applications. The enhanced binding is delocalized in nature, surrounding the whole surface of a charged fullerene, and is attributed to the polarization of the hydrogen molecules by the high electric field generated near the surface of the charged fullerene. At full hydrogen coverage, these charged fullerenes can gain storage capacities of up to  $\sim 8.0$  wt %. We also find that, contrary to intuitive expectation, fullerenes containing encapsulated metal atoms only exhibit negligible enhancement in the hydrogen binding strength, because the charge donated by the metal atoms is primarily confined inside the fullerene cages. These predictions may prove to be instrumental in searching for a new class of high-capacity hydrogen storage media.

Because of its abundance and environmentally friendly properties, hydrogen has been actively considered as an appealing alternative to fossil fuels for various energy applications. To possibly reach this eventual goal, one crucial issue is the availability of safe and efficient storage media.<sup>1</sup> Ideal hydrogen storage materials should have high gravimetric and volumetric densities, as specified by the targets of 6.0% mass ratio and 45 kg/m<sup>3</sup> volumetric capacity by 2010.<sup>2</sup> Other important criteria include the following: the binding energy should be about 0.2–0.6 eV per hydrogen molecule, so that hydrogen can adsorb and desorb under near ambient conditions,<sup>3</sup> and the hydrogen release should be reversible.

One class of candidate materials for high-capacity hydrogen storage is to use light-element-based materials with high surface areas, such as carbon nanotubes (CNTs) or other carbon-based nanostructures,<sup>4</sup> noncarbonaceous nanotubes,<sup>5,6</sup> and metal–organic frameworks.<sup>7</sup> Since the discovery of CNTs, their capacity as potential hydrogen storage media has been actively explored, and by now it has been generally agreed that pristine CNTs cannot effectively store hydrogen because the binding strength of molecular hydrogen on such

CNTs is too weak ( $\sim 0.03$  eV).<sup>8</sup> This is because the carbon nanotubes and fullerenes are quite stable structurally and very inert chemically, unable to interact strongly with molecular hydrogen, which itself is chemically rather inert. Several recent studies have shown that the binding strength of molecular hydrogen with nanoscaled carbon structures can be substantially enhanced by adsorption of transition metals such as Ti onto the surfaces,<sup>9,10</sup> but how to prevent the clustering of the adsorbed metal atoms remains a challenge.<sup>11,12</sup>

In this Letter, we explore systematically how charging of carbon fullerenes can affect their ability to bind molecular hydrogen, using first-principles calculations within density functional theory (DFT). We find that the binding strength of molecular hydrogen on either positively or negatively charged fullerenes  $C_n$  of different sizes ( $20 \leq n \leq 82$ ) can be substantially enhanced to 0.18–0.32 eV, a desirable range for potential room-temperature, near ambient applications. The enhanced binding is delocalized in nature, surrounding the whole surface of a charged fullerene, and is attributed to the polarization of the hydrogen molecules by the high electric field generated near the surface of the charged fullerene, which can gain storage capacities of up to  $\sim 8.0$  wt % at full hydrogen coverage. We further show that, contrary to intuitive expectation, fullerenes containing encapsulated metal atoms only exhibit negligible enhancement in hydrogen binding, because the charge donated by the metal

<sup>†</sup> Materials Science and Technology Division, Oak Ridge National Laboratory.

<sup>‡</sup> Department of Physics and Astronomy, The University of Tennessee.

<sup>§</sup> International Center for Quantum Structures and Institute of Physics, Chinese Academy of Sciences.

atoms is primarily confined inside the fullerene cages. These predictions are expected to be instrumental in searching for a new class of high-capacity hydrogen storage media.

Our DFT calculations were carried out using the Vienna ab initio simulation package (VASP),<sup>13</sup> with the exchange-correlation potential described by the Ceperley–Alder local density approximation (LDA)<sup>14</sup> as parametrized by Perdew and Zunger.<sup>15</sup> We employed the projector-augmented wave pseudopotentials.<sup>16</sup> The energy cutoff for the plane-wave basis set was 400 eV, and Monkhorst–Pack  $k$ -point sampling<sup>17</sup> was used for the integration. For selective cases, we also compared the LDA results with those containing nonlocal corrections to the exchange-correlation potential, as described by the Perdew–Wang version of the gradient generalized approximation (GGA).<sup>18</sup> For example, the binding energy of molecular hydrogen to a buckyball is 0.02 eV from GGA and 0.08 eV from LDA. On the other hand, it is known that GGA underestimates van der Waals interaction, as reflected by the observation that the graphite interlayer distance from LDA is 0.34 nm in good agreement with experiments, while it is greater than 0.4 nm from GGA. We therefore present mainly the LDA results.

In calculation of the energy of a charged cluster ( $C_n^q$ , with  $q$  being the net charge of a given fullerene of  $C_n$ ), a uniform background charge was introduced to keep the system charge neutral within a supercell.<sup>19</sup> The spurious electrostatic interactions due to the introduction of the uniform background charge, and that associated with the long-range interaction between different supercells, were corrected with monopole and multipole terms using the schemes implemented in VASP.<sup>19–21</sup> We have carefully monitored each correction component with respect to the supercell size, and energy convergence for each case has been confirmed. Positively charged fullerenes exhibit better energy convergence than negatively charged ones, because it is more difficult to treat a negatively charged system in a supercell calculation due to the highly diffusive nature of the extra electrons.<sup>22</sup> For example, we observed that energy levels stemming from fictitious states appear near the Fermi level as a fullerene is charged with more than two to four electrons depending on the size of the fullerene. Such fictitious states, corresponding to spatial distribution of electrons in the vacuum region, cause unphysical behaviors of the highly negatively charged fullerenes. In contrast, no such problems were observed for the positively charged fullerenes for  $q$  up to six holes. We therefore limit our investigation to systems  $C_n^q$  with  $-2 \leq q \leq +6$ .

The hydrogen binding strength to an  $sp^2$  carbon structure is primarily determined by the local curvature at a given binding site. Therefore, a fullerene whose local curvature is determined by its radius and the local bonding arrangement is an ideal model system to investigate  $H_2$  interaction with an  $sp^2$  carbon structure of various curvatures. For example, the  $H_2$  binding energy to a given fullerene is similar to that of a nanotube with a similar curvature and the energy converges to that of a graphene as the radius of the fullerene increases. In this study, we mainly consider a free floating fullerene because of its simplicity and theoretical conven-

ience. The use of such a representative system allows demonstration of how charging can modify the  $H_2$  interaction with an  $sp^2$  carbon material. The results obtained in this study are also qualitatively valid for other  $sp^2$  carbon materials of different form. Future studies may consider more sophisticated structures in order to get quantitative results for potential practical purposes.

A wide range of all-carbon fullerenes have been considered in the present study, including  $C_n$  with different symmetries:  $n = 60$  ( $I_h$ ), 72 ( $D_{6d}$ ), 74 ( $D_{3h}$ ), 76 ( $T_d$ ), and 82 ( $C_{2v}$ ). Smaller systems such as  $n = 20$  ( $I_h$ ), 28 ( $T_d$ ), 32 ( $C_2$ ), and 50 ( $D_{5h}$ ) have also been considered. Those small structures cannot satisfy the isolated pentagon rule<sup>23</sup> and are thus less stable (with lower cohesive energies per carbon atom). Correspondingly, the hydrogen binding to a pentagon on such a fullerene is stronger, because the electrons in neighboring pentagon(s) can help to enhance the binding. In particular,  $C_{20}$ , which completely consists of pentagons, is chemically so active that the adsorption of a hydrogen molecule onto its surface is dissociative. We exclude consideration of such highly reactive fullerenes as potential hydrogen storage media, because the atomic binding of H is too strong.

There are several ways to control the charging state of fullerenes, including electrochemical doping, ion/electron impact, laser desorption, and chemical doping. First, it has been demonstrated experimentally that electrochemical doping of fullerenes can lead to the formation of anions ( $q < 0$ ) or cations ( $q > 0$ ).<sup>24</sup> For instance,  $C_{60}$  and  $C_{70}$  fullerenes with irreversible charging of up to  $\pm 6$  electrons have been obtained in solution.<sup>24</sup> Second, using ion/electron bombardment<sup>25</sup> or laser desorption,<sup>26</sup> fullerene ions can be generated in gas phase. Third, chemical doping of fullerenes is another way to achieve various fullerene ions of high charge states; here doping can be substitutional, endohedral, exohedral doping, or via functionalization.<sup>24,27,28</sup> Substitutional doping of fullerenes can easily change their charge states.<sup>27</sup> Other charging methods include doping endohedrally or exohedrally by introducing metal atoms, ions, or charge-transfer complexes.<sup>24,28</sup> In particular, when metal atom(s) are encapsulated inside a hollow carbon cage to form a metallofullerene, substantial charge transfer from the metal atoms to the fullerene can take place. For example, charge transfer of up to six electrons has been observed experimentally when two La atoms were encapsulated in  $C_{80}$ .<sup>28</sup> In this study we will first focus on hydrogen binding to electronically doped fullerenes  $C_n^q$  and metallofullerenes consisting of a La atom encapsulated inside a fullerene ( $La@C_n$ ). We will also discuss the results in comparison with other related studies involving charging of fullerenes via other chemical doping methods.<sup>24–28</sup>

Figure 1a shows the binding energy of a single hydrogen molecule on charged fullerenes  $C_n^q$  as a function of charging state  $q$  for  $n = 28, 32, 60$ , and 82. When compared to the cases of neutral fullerenes, the molecular binding energy is enhanced by a factor of 2–5 as  $q$  changes from  $-2$  to  $+6$ . For example, the binding energy on  $C_{28}^{4+}$  is  $\sim 0.32$  eV, increased from  $\sim 0.06$  eV for binding on a neutral  $C_{28}$

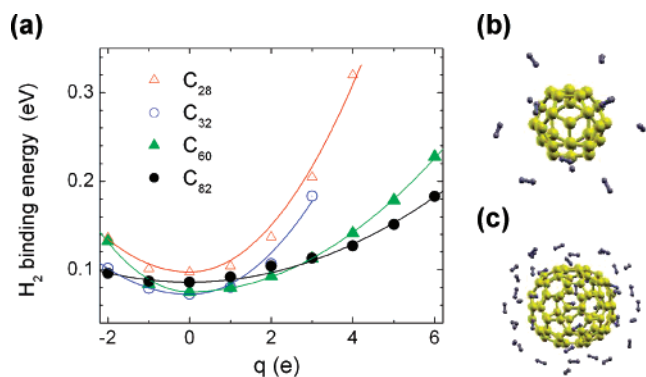


**Figure 1.** (a) Binding energy of molecular hydrogen on charged or neutral fullerenes. The DFT calculations (data points) are compared with semiclassical calculations (solid lines), and for both cases the binding energy increases quadratically with the net charge. (b, c) Structurally optimized hydrogen–fullerene complexes of (b)  $12\text{H}_2\text{--C}_{28}^{3+}$  and (c)  $43\text{H}_2\text{--C}_{82}^{6+}$ , with a hydrogen uptake of 6.67 wt % and 8.04 wt %, respectively.

fullerene. In addition, for a given host of  $\text{C}_n^q$ , the hydrogen adsorption geometry has been fully optimized at the center of a hexagonal carbon ring, where the binding is the strongest. The results show that the axis of the  $\text{H}_2$  molecule is aligned parallel to the surface of a positively charged fullerene but perpendicular to that of a negatively charged fullerene.

We next increase the coverage of hydrogen molecules on the charged fullerenes, using  $\text{C}_{28}^{3+}$  and  $\text{C}_{82}^{6+}$  as selective examples. Three hydrogen molecules can be adsorbed onto one hexagon of  $\text{C}_{28}^{3+}$ , residing on alternating tops of the atoms belonging to the hexagon. Depending on the relative orientations of the molecular axis, the binding energies differ substantially, equal to 0.41 eV per molecule when it is nearly vertical to the fullerene surface and 0.18 eV per molecule when it is nearly parallel. Because a  $\text{C}_{28}^{3+}$  fullerene has four hexagons, it can store at least 12 hydrogen molecules, giving rise to a hydrogen uptake of 6.67 wt % and a nearly constant binding energy of 0.19 eV per  $\text{H}_2$ . The optimized structure of 12  $\text{H}_2$  on  $\text{C}_{28}^{3+}$  is shown in Figure 1b, in which the distance of each molecule from the fullerene surface is also nearly a constant. Here we note that the 6.67 wt % is the lower capacity bound of a  $\text{C}_{28}^{3+}$  fullerene for hydrogen storage. It is possible that some additional hydrogen molecules could be adsorbed onto the  $(12\text{H}_2 + \text{C}_{28}^{3+})$  complex, albeit likely with somewhat weaker binding strengths. Figure 1c shows the optimized structure of 43  $\text{H}_2$  stored on  $\text{C}_{82}^{6+}$ , with one molecule per facet; the average binding energy per molecule is 0.18 eV, with little variations from molecule to molecule. The  $(43\text{H}_2 + \text{C}_{82}^{6+})$  complex corresponds to a lower capacity bound of 8.04 wt % for hydrogen storage. Because the average binding strength of the hydrogen molecules on these charged fullerenes is similar to that of a single  $\text{H}_2$  and is  $\sim 0.2$  eV, such charged fullerenes are promising candidates as high-capacity hydrogen storage media for applications under ambient conditions.<sup>29</sup>

To elucidate the underlying physical reason(s) for the enhanced binding of molecular hydrogen, we contrast in Figure 2a the electric fields generated by neutral and charged

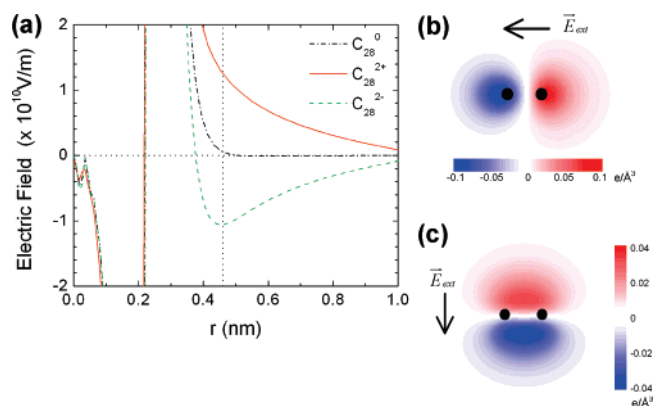


**Figure 2.** (a) Electric fields associated with neutral and charged fullerenes,  $\text{C}_{28}^q$  ( $q = -2, 0, +2$ ), at the center of a hydrogen molecule located on top of a hexagonal ring. (b, c) Charge density variations of a hydrogen molecule induced by an electric field of  $2 \times 10^{10}$  V/m applied (b) parallel and (c) perpendicular to the molecule axis, respectively.

fullerenes,  $\text{C}_{28}^q$  ( $q = -2, 0, +2$ ), along the radial direction from the center of the fullerene to that of a hydrogen molecule located on top of a hexagon. The radius of  $\text{C}_{28}$  is  $\sim 0.24$  nm, and the hydrogen molecule is located at 0.46 nm from the center, as indicated by the vertical dotted line. The optimum hydrogen binding site is initially determined by the van der Waals interaction between  $\text{H}_2$  and a neutral fullerene and further stabilized by its polarization under the electric field surrounding a charged fullerene. The electric field experienced by  $\text{H}_2$  is negligible on a neutral  $\text{C}_{28}$ , but on a charged fullerene it is enhanced to  $\sim 1.5 \times 10^{10}$  V/m at the hydrogen site. Figure 2 illustrates the charge density redistribution of a hydrogen molecule under a strong electric field of  $2 \times 10^{10}$  V/m applied along either (b) parallel or (c) perpendicular direction to the molecular axis. The resulting electric dipole moment ( $\vec{p}$ ) is given by  $\vec{p} = \alpha \vec{E}_{\text{ext}}$ , where  $\alpha$  is the electric polarizability of the molecule. The corresponding energy decrease is  $\Delta U = -1/2 \vec{p} \cdot \vec{E}_{\text{ext}}$ ,<sup>30</sup> which is largely responsible for the enhanced hydrogen–fullerene binding. The polarizability along ( $\alpha_{\parallel}$ ) and perpendicular ( $\alpha_{\perp}$ ) to the hydrogen axis is 6.3 (a.u.) and 4.85 (a.u.), respectively.<sup>31</sup> Therefore, an electric field of  $\sim 2 \times 10^{10}$  V/m generated by a charged fullerene will result in a hydrogen binding energy of  $\sim 0.2$  eV. The hydrogen binding energy to a charged fullerene estimated by this semiclassical approach (solid lines in Figure 1a) is in good agreement with the DFT results (data points in Figure 1a), both showing a quadratic increase with the net charge. It should be noted that the semiclassical picture is applicable only if the hydrogen orbitals have no strong hybridization with that of a fullerene.

When a fullerene molecule is too highly charged, the strong electric field will dissociate a hydrogen molecule during structure optimization, as indicated by the missing certain data points in Figure 1a. The critical field  $E_{\text{ext}}^c$  above which hydrogen dissociation would occur is determined by the dissociation barrier of a hydrogen molecule on a fullerene. Here, as the strength of electric field increases, the barrier decreases and finally vanishes at  $E_{\text{ext}}^c$ , whose precise value varies from fullerene to fullerene.

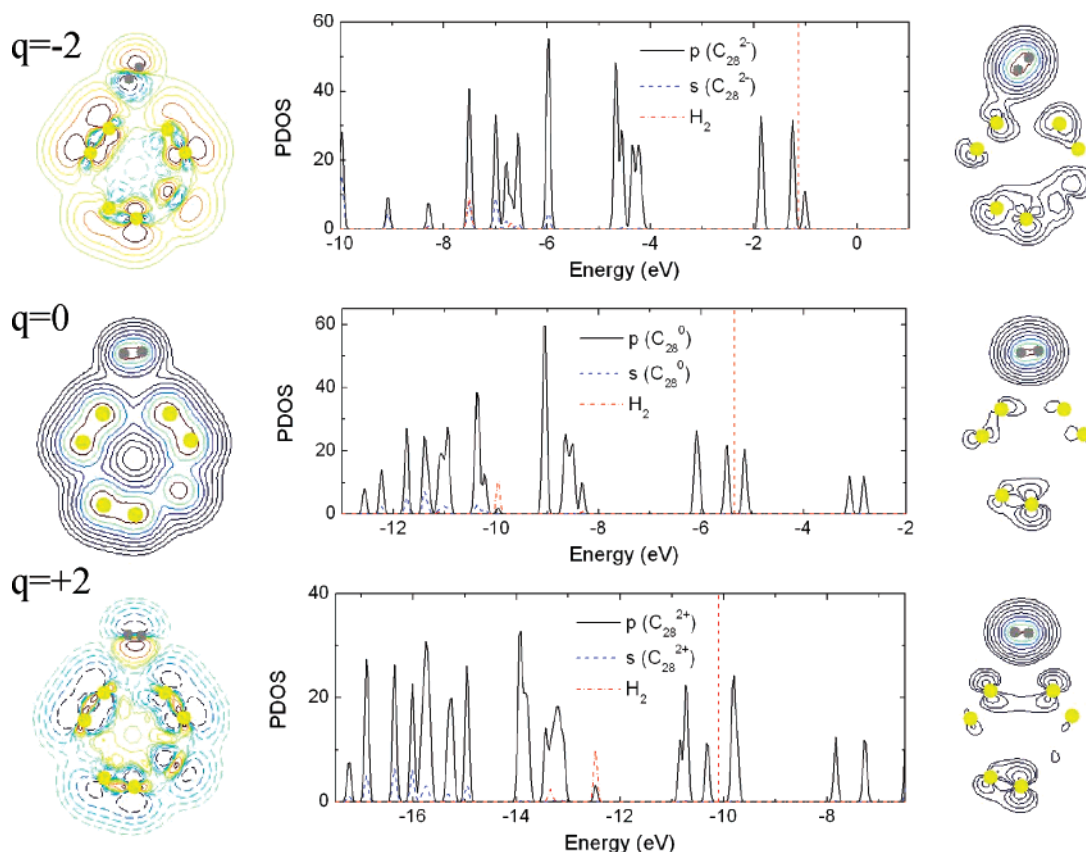


**Figure 3.** Left column: charge density of the complexes  $\text{H}_2\text{-C}_{28}^{2-}$  (upper panel),  $\text{H}_2\text{-C}_{28}^0$  (middle panel), and  $\text{H}_2\text{-C}_{28}^{2+}$  (lower panel), with the hydrogen molecule located at the center of a hexagonal ring. For the charged cases, only the charge density differences are displayed, measured relative to the densities of the corresponding neutral complexes with frozen atomic geometries as the fully optimized ones for the charged complexes. For the neutral case, the total charge density is displayed. The middle column displays the partial densities of states, where the Fermi levels are indicated by the dotted red lines. The charge densities of the levels involved in hydrogen bonding to the fullerene are shown in the right column.

Next we analyze the detailed charge redistributions of neutral or charged fullerenes upon  $\text{H}_2$  adsorption. The left column of Figure 3 shows the charge densities of the  $\text{H}_2\text{-C}_{28}^q$  ( $q = -2, 0, +2$ ) complexes, where the hydrogen molecule is located at the center of a hexagonal ring. For the charged cases, only the charge density differences ( $\Delta\rho$ ) are displayed, measured relative to the densities of the corresponding neutral complexes with frozen atomic geometries as the fully optimized ones for the charged complexes. For the neutral case, the total charge density ( $\rho$ ) is displayed.

The optimized geometries show that  $\text{H}_2$  aligns parallel to the surface of a positively charged fullerene, while a perpendicular configuration is preferred on a negatively charged fullerene. The different orientation preference is mainly due to the interaction between the quadrupole moment of  $\text{H}_2$  and the gradient of the external field.<sup>32</sup> Within a good approximation, the Hamiltonian of the  $\text{H}_2$  molecule under an external electric field can be expressed in terms of the unperturbed Hamiltonian plus interaction terms of dipolar and quadrupolar nature. At the optimum  $\text{H}_2$  location near a fullerene, the dipole term dominates, with  $\Delta U = -1/2 \vec{p} \cdot \vec{E}_{\text{ext}}$ . The next-order term ( $\Delta U'$ ) contains the information about the orientation of the  $\text{H}_2$  molecule in terms of the sign of the charged object;  $\Delta U' = -1/2 Q \nabla E_{\text{ext}} P_2(\cos \theta)$ , where  $\theta$  is the orientation of the molecule with respect to a field in

radial direction,  $Q$  the quadrupole moment in the fixed-molecule frame, and  $P_2$  the Legendre polynomial.<sup>32</sup> In order to minimize the total energy up to second order in the multipole expansion, the  $\text{H}_2$  orientation of  $\theta = \pi/2$  (parallel to the fullerene surface) is obtained for a positively charged fullerene, while that with  $\theta = 0$  (perpendicular to the fullerene surface) is favorable for a negatively charged fullerene.

Next, the origin of the high electric field produced by a charged fullerene is explained on the level of quantum mechanics. Here we analyze the partial densities of states (PDOS) of the fullerenes and a hydrogen molecule on positively and negatively charged fullerenes in comparison with the neutral cases, as presented in the middle column of Figure 3. There is no significant change in the overall feature of the density of states (DOS) of the fullerenes when their charge states are varied; instead, such homogeneous charging only causes a rigid shift of the Fermi level (dashed red line), upward or downward by  $\sim 4.5$  eV for  $\text{C}_{28}^{2-}$  or  $\text{C}_{28}^{2+}$ , respectively. This observation is consistent with the changes in HOMO (highest occupied molecular orbital) and LUMO (lowest unoccupied molecular orbital) levels. When two electrons are added to the fullerene, the doubly degenerate HOMO level becomes triply degenerate, while the doubly degenerate LUMO becomes nondegenerate (upper panel in



the middle column). Similarly, the LUMO becomes triply degenerate and the HOMO nondegenerate when two electrons are removed from the fullerene (bottom panel). The rigid shift of the Fermi level of a charged fullerene effectively results in the macroscopic electric field ( $E_{\text{ext}}$ ); that is, as we bring  $\text{H}_2$  to the charged object, its Fermi level also shifts to match the new Fermi level and the global Fermi level will be determined in chemical equilibrium. As a result, the molecular hydrogen levels experience Stark effects<sup>31</sup> on the charged fullerenes and electronic hybridization with the fullerene states will take place accordingly. The charge differences  $\Delta\rho$  shown in the left column of Figure 3 exhibit high degrees of polarization of the hydrogen molecule under the high electric field produced by the charged fullerenes, resulting in the enhanced fullerene–hydrogen binding energies of  $\sim 0.14$  eV for  $\text{C}_{28}^{2+}$  and  $\text{C}_{28}^{2-}$ . In short, the quantum mechanical results from DFT calculations confirm quantitatively the semiclassical predictions on the difference in  $\text{H}_2$  orientation for the positively and negatively charged fullerenes, the charge redistribution and corresponding energy gain, and the strength of electric field generated by charged fullerenes from the point charge approximation.

On both positively and negatively charged fullerenes, a small spread of the  $\text{H}_2$   $\sigma$  state is observed, resulting in an upward or downward shift of the  $\text{H}_2$   $\sigma$  level by  $\sim 2.5$  eV with the addition or removal of two electrons. As a result, the fullerene  $\pi$  state is weakly involved in the hydrogen binding to the positively charged fullerene, while the  $\sigma$  state is involved in the binding to the negatively charged fullerene (see the right column of Figure 3). In the latter case, the hybridization is relatively stronger because of the perpendicular orientation of the adsorbed hydrogen molecule. The amount of transferred charge from the fullerene to  $\text{H}_2$  is negligible (less than 0.01 electrons), and a slight increase in the hydrogen bond length (up to 0.6%) is observed on the negatively doped fullerene.

We now compare the different and conceptually distinct approaches of enhancing the binding strength of  $\text{H}_2$  on functionalized fullerenes. One is to coat the fullerenes with reactive transition metals such as Ti.<sup>9,10</sup> The other is to dope the fullerenes substitutionally with other light elements of different valent states such as B.<sup>33</sup> As discussed in the introduction, for the first approach how to prevent clustering of the metal adatoms remains a challenge. Furthermore, for both approaches the active sites for enhanced binding are spatially localized around the adatoms or the dopants.<sup>9,10</sup> In contrast, the approach of using charged fullerenes proposed here establishes strong electric fields surrounding the whole surface of a fullerene; therefore, the enhanced binding is delocalized or global in nature, surrounding the whole surface of the charged fullerene.

Next, we briefly discuss the effectiveness of charging fullerenes by encapsulating different metal atoms inside the cages and the corresponding influence on the binding strength of  $\text{H}_2$  on such metallofullerenes. Various metal atoms have been encapsulated inside fullerenes experimentally,<sup>24,28</sup> and efficient charge transfer from the metal atoms to the fullerenes has been observed.<sup>24,28</sup> As an example, we focus

on metallofullerenes ( $\text{La@C}_n$ ) consisting of a single La atom encapsulated inside  $\text{C}_n$  ( $28 \leq n \leq 82$ ). We find that three electrons are transferred from La to the fullerenes for all the considered cases.<sup>24</sup> Nevertheless, the binding strength of  $\text{H}_2$  on  $\text{La@C}_n$  remains very weak, showing negligible enhancement over the binding strength on uncharged pristine fullerenes. This finding, somewhat counterintuitive, turned out to reflect the observation that the transferred charge is highly localized near the La ion and inside the fullerene cage, making the electric field of dipolar nature felt outside the cage relatively weak. Therefore, despite the existence of significant charge transfer, metallofullerenes are not promising materials as high-capacity hydrogen storage media.

Before closing, we briefly discuss potential experimental realization of charged fullerenes and validation of the strong predictions made in the present study. Electrochemical doping<sup>24</sup> generally works to produce fullerene ions because there are counterions nearby in the solution, but for such systems little free space for hydrogen adsorption is left. Using ion/electron bombardment<sup>25</sup> or laser desorption,<sup>26</sup> fullerene ions can be generated in gas phase, resulting in ideal model systems to test the effect of charging on the  $\text{H}_2$  binding strength. Here, the challenge is to produce large quantities of such charged fullerenes with good volumetric density for practical applications. Chemical doping is another way to achieve various fullerene ions of high charge states. Doping approaches include substitutional, endohedral, exohedral, and via functionalization.<sup>24,27,28</sup> By substitutional doping of a fullerene with elements such as B or N, the net number of electrons of a fullerene can be changed.<sup>27</sup> However, this approach creates charged fullerenes that are only locally chemically active for enhanced  $\text{H}_2$  binding, mediated by local charge transfer.<sup>33</sup> We found no noticeable electric field surrounding such objects. High charge transfer achieved by endohedral doping of fullerene failed to achieve a high electric field outside because of screening. On the other hand, exohedral doping and chemical functionalization are alternative ways to achieve fullerene anions or cations. It has been experimentally shown that additions of various elements such as alkali metal and alkaline earth species and charge-transfer complex such as TDAE (tetrakis-dimethylaminoethylene) can successfully produce fullerene ( $\text{C}_{60}$  and  $\text{C}_{70}$ ) anions.<sup>24</sup> Such a chemical reduction mechanism can be achieved relatively easily compared to that of oxidation of fullerenes due to their high electron affinity. The addition of a few F complexes to a fullerene or alkoxyated or arylated fullerene derivatives result in fullerene cations.<sup>24</sup> Homogeneous exohedral doping or functionalization using charge-transfer complexes could be promising ways to achieve fullerene anions and cations. Finally, the predicted strong enhancement in  $\text{H}_2$  binding on charged fullerenes can be at least partially validated using charged fullerene molecules adsorbed on a poorly conduction Si(100) surface.<sup>34</sup> Such an experiment is not only physically feasible but also worthwhile in its own right besides its relevance to the present work.

In summary, we have investigated systematically how charging of carbon fullerenes can affect their ability to bind molecular hydrogen using first-principles calculations. We

found that the binding strength of molecular hydrogen on either positively or negatively charged fullerenes can be substantially enhanced to 0.18–0.32 eV, a desirable range for potential room-temperature, near ambient applications. The enhanced binding is delocalized in nature, surrounding the whole surface of a charged fullerene, and is attributed to the polarization of the hydrogen molecules by the high electric field near the surface of the charged fullerene. At full hydrogen coverage, the charged fullerenes gain storage capacities of ~8.0 wt %. We have also shown that, contrary to initial intuitive expectation, fullerenes containing encapsulated metal atoms only exhibit negligible enhancement in hydrogen binding, because the charge donated by the metal atoms is primarily confined inside the fullerene cages. These predictions are expected to motivate active research efforts to search for potential new high capacity hydrogen storage media.

**Acknowledgment.** We thank Dr. R. N. Compton and Dr. D. B. Geohegan for helpful discussions. This work was supported by the U.S. DOE (Grant No. DEFG0205ER46209, and the Division of Materials Sciences and Engineering, Office of Basic Energy Sciences, DOE, under Contract DE-AC05-00OR22725 with Oak Ridge National Laboratory, managed by UT-Battelle, LLC), supplemented by the U.S. NSF (grant no. DMR-0606485) and the NSF of China. The calculations were performed at ORNL's Center for Computational Sciences and at the National Energy Research Scientific Computing Center (NERSC).

## References

- Schlapbach, L.; Züttel, A. *Nature* **2001**, *414*, 353. Schüth, F.; Bogdanović, B.; Felderhoff, M. *Chem. Commun.* **2004**, 2249. Seayad, A. M.; Antonelli, D. M. *Adv. Mater.* **2004**, *16*, 765.
- <http://www.eere.energy.gov/hydrogenandfuelcells/>.
- Li, J.; Furuta, T.; Goto, H.; Ohashi, T.; Fujiwara, Y.; Yip, S. *J. Chem. Phys.* **2003**, *119*, 2376.
- Züttel, A.; Sudan, P.; Mauron, Ph.; Kiyobayashi, T.; Emmenegger, Ch.; Schlapbach, L. *Int. J. Hydrogen Energy* **2002**, *27*, 203.
- Tang, C.; Bando, Y.; Ding, X.; Qi, S.; Golberg, D. *J. Am. Chem. Soc.* **2002**, *124*, 14550; Chen, J.; Li, S.-L.; Tao, Z.-L.; Shen, Y.-T.; Cui, C.-X. *J. Am. Chem. Soc.* **2003**, *125*, 5284.
- Meng, S.; Kaxiras, E.; Zhang, Z. *Nano Lett.* **2007**, *7*, 663.
- Rosi, N. L.; Eckert, J.; Eddaoudi, M.; Vodak, D. T.; Kim, J.; O'Keeffe, M.; Yaghi, O. M. *Science* **2003**, *300*, 319.
- Ye, Y.; Ahn, C. C.; Witham, C.; Fultz, B.; Liu, J.; Rinzler, A. G.; Colbert, D.; Smith, K. A.; Smalley, R. E. *Appl. Phys. Lett.* **1999**, *74*, 2307. Gordon, P. A.; Saeger, R. B. *Ind. Eng. Chem. Res.* **1999**, *38*, 4647.
- Yildirim, T.; Ciraci, S. *Phys. Rev. Lett.* **2005**, *94*, 175501. Yildirim, T.; Iniguez, J.; Ciraci, S. *Phys. Rev. B* **2005**, *72*, 153403.
- Zhao, Y.; Kim, Y.-H.; Dillon, A. C.; Heben, M. J.; Zhang, S. B. *Phys. Rev. Lett.* **2005**, *94*, 155504.
- Zhang, Y.; Dai, H. *Appl. Phys. Lett.* **2000**, *77*, 3015.
- Sun, Q.; Wang, Q.; Jena, P.; Kawazoe, Y. *J. Am. Chem. Soc.* **2005**, *127*, 14582.
- Kresse, G.; Furthmüller, J. *Phys. Rev. B* **1996**, *54*, 11169.
- Ceperley, D. M.; Alder, B. J. *Phys. Rev. Lett.* **1980**, *45*, 566.
- Perdew, J. P.; Zunger, A. *Phys. Rev. B* **1981**, *23*, 5048.
- Blöchl, P. E. *Phys. Rev. B* **1994**, *50*, 17953. Kress, G.; Joubert, D. *Phys. Rev. B* **1999**, *59*, 1758.
- Monkhorst, H. J.; Pack, J. D. *Phys. Rev. B* **1976**, *13*, 5188.
- Perdew, J. P.; Wang, Y. *Phys. Rev. B* **1992**, *45*, 13 244.
- Makov, G.; Payne, M. C. *Phys. Rev. B* **1995**, *51*, 4014.
- Neugebauer, J.; Scheffler, M. *Phys. Rev. B* **1992**, *46*, 16067.
- Kresse, G.; Furthmüller, J. *VASP the Guide*; Vienna University of Technology: Vienna, 1999; Chapter 8.6, <http://cms.mpi.univie.ac.at/VASP/>.
- The different behaviors between positively and negatively charged systems in supercell calculations were discussed previously. For example, see: Shim, J.; Lee, E.-K.; Lee, Y. J.; Nieminen, R. M. *Phys. Rev. B* **2005**, *71*, 035206. Balamurugan, D.; Prasad, R. *Phys. Rev. B* **2006**, *73*, 235415.
- Schmalz, T. G.; Seitz, W. A.; Klein, D. J.; Hite, G. E. *Chem. Phys. Lett.* **1986**, *130*, 203. Klein, D. J.; Schmalz, T. G.; Hite, G. E.; Seitz, W. A. *J. Am. Chem. Soc.* **1986**, *108*, 1301.
- Dresselhaus, M. S.; Dresselhaus, G.; Eklund, P. C. *Science of Fullerenes and Carbon Nanotubes*; Academic Press: San Diego, CA, 1996.
- Walch, B.; Cocke, C. L.; Voelpel, R.; Salzborn, E. *Phys. Rev. Lett.* **1994**, *72*, 1439. Jin, J.; Khemliche, H.; Prior, M. H. *Phys. Rev. A* **1996**, *53*, 615.
- Hettich, R. L.; Compton, R. N.; Ritchie, R. H. *Phys. Rev. Lett.* **1991**, *67*, 1242.
- Xie, R.-H.; Bryant, G. W.; Zhao, J.; Smith, V. H.; Di Carlo, A.; Pecchia, A., Jr. *Phys. Rev. Lett.* **2003**, *90*, 206602.
- Shinohara, H. *Rep. Prog. Phys.* **2000**, *63*, 843.
- A previous study based on classical interaction potentials showed that charged single wall carbon nanotubes are not suitable materials for hydrogen storage under ambient conditions unless unrealistically high charges are imposed on the tubes. See: Simonyan, V. V.; Diep, P.; Johnson, J. K. *J. Chem. Phys.* **1999**, *111*, 9778.
- Jackson, J. D. *Classical Electrodynamics*; John Wiley: New York, 1975.
- Mura, M. E.; Smith, D. A. *Chem. Phys. Lett.* **1993**, *203*, 578 and references therein. Saika, A.; Musher, J. I.; Ando, T. *J. Chem. Phys.* **1970**, *53*, 4137.
- Poll, J. D.; Hunt, J. L. *Can. J. Phys.* **1985**, *63*, 84.
- Kim, Y.-H.; Zhao, Y.; Williamson, A.; Heben, M. J.; Zhang, S. B. *Phys. Rev. Lett.* **2006**, *96*, 016102.
- Gensterblum, G.; Pireaux, J. J.; Thiry, P. A.; Caudano, R.; Vigneron, J. P.; Lambin, Ph.; Lucas, A. A.; Krätschmer, W. *Phys. Rev. Lett.* **1991**, *67*, 2171.

NL070809A